



Article

Novel PolyPropylene–*Sargassum* Particles Composites: Evaluation of Thermal and Thermomechanical Properties

Jesús Daniel Aragón-Vallejo ¹, Beatriz Adriana Salazar-Cruz ¹, María Yolanda Chávez-Cinco ¹, José Luis Rivera-Armenta ^{1,*} and Ana Cecilia Espindola-Flores ²

¹ Instituto Tecnológico de Ciudad Madero, Tecnológico Nacional de México, Prol. Bahía de Aldahir y Av. de las Bahías S/N Parque de la Pequeña y Mediana Industria, Altamira 89600, Tamaulipas, Mexico

² Instituto Politécnico Nacional, Altamira 89600, Tamaulipas, Mexico

* Correspondence: jlriveraarmenta@itcm.edu.mx; Tel.: +52-833-5342961

Abstract: *Sargassum* is a type of marine algae that has caused environmental problems in Mexico because it arrives in high quantities along the Mexican coast, especially in the Mexican Caribbean. This situation has become an environmental and economic problem, impacting tourism and other activities. As a result, it is reasonable to try to find an application for these algae. Recently, some applications in civil construction, cosmetics, and the food industry, among others, have been reported. The present work evaluates the thermal and structural properties of new polypropylene (PP)–*Sargassum*-based composites. Also, the effect of adding calcium stearate (CS) to increase the interaction between PP and *Sargassum* particles was investigated. PP–*Sargassum* particle composites were prepared by a melt mixing process, and the properties of these composites were evaluated using thermal techniques such as dynamic mechanical analysis (DMA), thermogravimetric analysis (TGA), differential scanning calorimetry (DSC), X-ray diffraction (XRD), and infrared spectroscopy (FTIR). The DMA results showed that composites with low concentrations of *Sargassum* particles perform better than those with higher concentrations. When CS was added to composites, there was a significant improvement in storage modulus compared with composites without CS. This was attributed to the good adhesion of the particles to the matrix because the mobility of macromolecules increased in the presence of CS. The thermal stability of PP–*Sargassum* particle composites decreases when the amount of particles increases, and the addition of CS does not positively affect the thermal behavior of composites. The findings open the possibility of using *Sargassum* particles in new applications of these algae as a polymer additive to generate sustainable materials.

Keywords: *Sargassum*; calcium stearate; biomaterials; polymeric composites; crystallinity



Citation: Aragón-Vallejo, J.D.; Salazar-Cruz, B.A.; Chávez-Cinco, M.Y.; Rivera-Armenta, J.L.; Espindola-Flores, A.C. Novel PolyPropylene–*Sargassum* Particles Composites: Evaluation of Thermal and Thermomechanical Properties. *J. Compos. Sci.* **2023**, *7*, 455. <https://doi.org/10.3390/jcs7110455>

Academic Editors: Deesy Gomes Pinto and Rajashekhar Kurahatti

Received: 13 September 2023

Revised: 30 September 2023

Accepted: 20 October 2023

Published: 1 November 2023



Copyright: © 2023 by the authors. Licensee MDPI, Basel, Switzerland. This article is an open access article distributed under the terms and conditions of the Creative Commons Attribution (CC BY) license (<https://creativecommons.org/licenses/by/4.0/>).

1. Introduction

In recent years, the use of lignocellulosic materials has generated growing interest not only in the search to take advantage of materials that do not have an application for industrial applications but also as an option to improve the physicochemical properties of different types of matrices, with polymers being the most studied materials. One of the reasons to search for applications for lignocellulosic materials from natural origin is to produce sustainable materials that use these kinds of renewable materials. Some areas that have captured interest are applications of lignocellulosic materials in composites such as in the automotive industry, pavements, the construction industry, furniture, and packing. Also, several research groups have studied the mechanical properties of polymer composites filled with agricultural residues [1–8]. The fabrication of advanced composites with organic materials can generate excellent strength and thermal and moisture resistance. Although natural fibers cannot provide as much strength as synthetic fibers, they can achieve an acceptable strength level.

Natural fibers mainly consist of cellulose, hemicelluloses, pectin, lignin, and some other polysaccharides. In addition to their biodegradability and renewability, natural fibers and

powders are cheaper, lighter, and more resistant per unit mass than typical inorganic fillers. There are examples of lignocellulosic fillers or reinforcers from multiple origins, such as sugarcane bagasse, jute, sisal, hemp, cotton, rice husks, cocoa pod husks, hazelnut shells, and wood. These materials from biomass can be introduced into various thermoplastic polymers, such as polyvinyl chloride (PVC), polylactic acid, polyethylene, and PP, and thermosetting resins, such as polyesters and epoxy resins and rubbers. Reference [2] reports improvements in physicochemical properties and, in some cases, biodegradation characteristics.

The genus *Sargassum* has received increasing attention since 1985 due to the accumulation of growth on the Caribbean coasts that arrives from the north equatorial Atlantic and coast of Africa. This kind of algae has four subgenera: *Sargassum*, *Arthrophyucus*, *Bactrophyucus*, and *Phyllotrichia*. The subgenus *Sargassum* is the most diverse subgenus, and it is divided into three sections: *Zygocarpicae*, *Malacocarpicae*, and *Acanthocarpicae*. In Mexico, there are two species of *Sargassum*, *S. fluitans* and *S. natans*, which are the most abundant in the Mexican Caribbean and Gulf of Mexico. Governments have taken the initiative to minimize the damage caused by these algae due to the serious environmental damage and the considerable impact on the tourism industry. Due to the above, several research groups have sought options for using this type of algae. The extraction of nanocellulose and civil construction are the most explored areas, and even domestic areas, such as fertilizers and the food industry, have also been reported [9,10]. Despite the use of *Sargassum* by some research groups, there has not been any recorded use of *Sargassum* in Tamaulipas, Mexico. *Sargassum* is mainly composed of cellulose, hemicellulose, lignin, and considerable amounts of alginate, components that have a high degree of crystallinity [11,12]. Recently, the use of *Sargassum* as an additive in a styrene–butadiene–styrene (SBS) copolymer matrix was reported by our research group. We found an improvement in the mechanical properties, which can be an opportunity to use this kind of algae as a bio-additive for composites in the shoe industry [13].

The mechanical properties of a composite depend on the filler/matrix interface. This interface can be improved with the addition of coupling agents or by using surface treatments [14–18]. Calcium stearate (CS) is a chemical product that is mainly used as a slip agent in PVC. Also, it is a lubricating agent, an acid scavenger or neutralizer, and a release agent in other kinds of polymers, including polyolefins. CS has already been used as an additive in previous studies of polyolefins, and references [19,20] reported an improvement in the wear resistance and the tensile and thermal properties of materials, but it has not been used to enhance stiffness or rigidity. According to FTIR results, other researchers report that CS acts as a pro-oxidant and generates chemical changes in PP resin when exposed to environmental conditions [21]. Other work reports using CS as a soap, and positive results were obtained. Also, an interesting dissociation of an ionic cluster, modifying the crystallinity behavior, was reported when PP was heated [22]. Most reports used CS as a lubricant or surfactant to improve the compatibility of CaCO₃ and PP. However, there are no reports of using this additive with lignocellulosic materials.

The main problem with using natural fibers or particles is their nature. Thermoplastic polymers are hydrophobic, and natural materials are hydrophilic. However, there are several ways to improve their interaction. One of the most used is the chemical treatment of the fibers or the polymeric matrix. For lignocellulosic materials, a treatment with basic solutions is a good option [23]. In the case of polymers, a graft reaction on polyolefins and maleic anhydride modification, or a combination of both options, have been reported. Using a combination of CS and grafted PP with maleic anhydride improved the mechanical properties of the composites [24]. In another work, the effect of CS-coated CaCO₃ nanoparticles on the crystallization process was reported, and it was found that a nucleating effect generated by a monolayer causes an increase in crystallinity [25]. The use of other ester additives was reported to have a positive effect on the crystallinity of PP [26]. The use of silane compounds as graft additives was also reported to improve the interaction between the natural materials and the polymer matrix because there is a better interfacial interaction

between materials. This positively affected tensile strength, tensile modulus, and impact properties, among others [27].

In the present investigation, we report using *Sargassum* particles in a PP matrix and evaluate the thermal properties of PP–*Sargassum* composites. Also, CS was added with the aim of improving the interaction between *Sargassum* particles and PP. The PP–*Sargassum* composites were prepared by a melt-mixing process, and the composite properties were evaluated by means of DMA, FTIR, TGA, DSC, and XRD.

2. Materials and Methods

2.1. Materials

Sargassum (*S. nattans* kind) was collected from Miramar Beach in the city of Madero, Tamaulipas. The algae were repeatedly washed with water to remove salts and other impurities. Subsequently, the *Sargassum* was dried for a day. Once dry, it was ground by milling with an IKA A11 Analytical (Wilmington, NC, USA) and sieved with a #80 mesh screen (JPLAB, Guangzhou, China) to obtain a homogeneous particle size of 177 microns. Calcium stearate (CS) was obtained from Quimica Suastes, S.A. de C.V. (Mexico City, Mexico), Polypropylene Profax[®] was donated by Indelpro S.A. de C.V. (Altamira, Mexico). The polymer density was 0.9 g/cm³ with a melt flow index of 25 g/10 min (according to ASTM D1238).

2.2. Composite Preparations

The PP–*Sargassum* particle composites were prepared using a Brabender plastograph (Diusburg, Germany) internal mixer with roller blades. The PP, *Sargassum* particles, and CS were mixed in a tray, and the composites were mixed for 15 min at 80 rpm and 180 °C. Table 1 reports the *Sargassum* particle contents in composites from 2 to 10 phr (parts per hundred of resin) and the codes used for sample identification. The CS content was kept fixed at 1% wt. Then, the blend was molded by a compression process in a hydraulic press (DAKE, Grand Haven, MI, USA) at 215 °C with a ramp of 0, 5, and 10 tons, with 5 min for each step. Finally, the samples were allowed to cool down to room temperature for another 5 min; then, samples were taken for each characterization.

Table 1. Composition and nomenclature of PP–*Sargassum* particle and PP–*Sargassum* particle–CS composites.

<i>Sargassum</i> Particle Concentration	Unmodified	Modified with CS
0 PHR *		PP
2 PHR *	PP-2S	PP-2S-CS
4 PHR *	PP-4S	PP-4S-CS
6 PHR *	PP-6S	PP-6S-CS
8 PHR *	PP-8S	PP-8S-CS
10 PHR *	PP-10S	PP-10S-CS

* PHR: parts per hundred of resin.

2.3. Composite Characterization Methods

FTIR analysis was conducted using an infrared spectrometer, Perkin Elmer (Waltham, MA, USA) Spectrum One model, equipped with an attenuated total reflectance (ATR) accessory with a ZnSe plate. The analyses were recorded with 12 scans in the wavelength range from 4000 to 600 cm^{−1} with a resolution of 4 cm^{−1}.

A DMA test was performed using DMA equipment, TA Instruments (New Castle, DE, USA) Q800 model, using a dual cantilever clamp. The temperature range evaluated was from −40 °C to 150 °C, and an ACS3 accessory was used for cooling; the heating rate was 5 °C/min with a frequency of 1 Hz.

TGA was carried out using a TA Instruments (New Castle, DE, USA) model Q600. The sample weight was about 10 ± 2 mg, platinum crucibles were used, and the temperature range was from 30 to 600 °C, with a heating rate of 10 °C/min under a nitrogen atmosphere with a flow rate of 100 mL/min.

DSC characterization was conducted using a Perkin Elmer (Waltham, MA, USA) model DSC 8000. The sample size was about 10 ± 2 mg, and sealed aluminum pans were used. The samples were first heated from -20 to 250 °C with a heating rate of 20 °C/min and then kept at 250 °C for 5 min. After that, a cooling step was carried out at a rate of 20 °C/min until -20 °C was reached. Then, the sample was kept for another 5 min at this temperature. Finally, a heating process was carried out from -20 to 250 °C with a heating rate of 10 °C/min. The data collected (ΔH_m and T_m) from this cycle were used to calculate the degree of crystallinity (X_c) using Formula (1):

$$X_c = (\Delta H_m / \Delta H^\circ) \times 100 \quad (1)$$

where ΔH_m is the melting enthalpy per mass unit of PP, calculated from the area under the melting peak for PP and the composites. ΔH° is the melting enthalpy per mass unit of the 100% crystalline PP; it has a value of 207 J/g [3].

XRD characterization was conducted using a Bruker diffractometer (Billeric, MA, USA), D8 Advance model. The scan range was between 5 and 40 degrees on a 2θ scale with $\text{CuK}\alpha$ radiation ($\lambda = 0.15405$ nm). The equipment was operated at 40 kV and 40 mA at a rate of 0.02 s $^{-1}$. The crystallinity degree was calculated from XRD data by considering the total crystalline and amorphous areas of the diffractogram according to Equation (2):

$$X_c = [A_c / (A_c + A_a)] \times 100\% \quad (2)$$

where A_c represents the area of crystalline peaks and A_a represents the area of the amorphous phase in PP and composites.

3. Results

3.1. Characterization by FTIR

Figure 1a shows the FTIR spectra of PP, PP-2S, and PP-10S composites. The aim was to evaluate the effect of low and high *Sargassum* particle content. The IR spectra for all the prepared composites are included in Supplementary Information (Figures S3 and S4). In the PP IR spectra, it is possible to identify the characteristic signals attributed to the backbone of the polymer: C-H stretching at 3000 – 2800 cm $^{-1}$, $-\text{CH}_2$ bending at 1450 cm $^{-1}$, and $-\text{CH}_3$ bending and symmetric deformations at 1370 and 1160 cm $^{-1}$ [28–30]. Also, for PP-2S and PP-10S composite spectra, in addition to the signals attributed to PP, it is possible to identify the presence of signals attributed to OH and C=O groups at 1700 and 1630 cm $^{-1}$ and at 1260 cm $^{-1}$ from carboxylic groups present in hemicellulose, cellulose, and lignin present in *Sargassum* signals. This corroborates the presence of *Sargassum* particles in the PP matrix [29–32].

On the other hand, the FTIR spectra of PP, PP-2S-CS, and PP-10S-CS composites are depicted in Figure 1b, which shows the same signals as PP–*Sargassum* without CS, but the peak at 1750 cm $^{-1}$, attributed to C=O group of hemicellulose, alginate, lignin, and cellulose present in *Sargassum* [29–32], shows higher intensity, which can be associated with a greater presence of those compounds. Another signal that became more evident is the peak around 1600 cm $^{-1}$, which can be associated with a carboxylate signal from alginate, which is present in *Sargassum* [29,33]. In addition, the peak attributed to the OH groups (3300 cm $^{-1}$) becomes more evident in composites with CS. This can be related to the presence of *Sargassum* particles in the PP matrix, corroborating the benefit of adding CS because there is a better interaction between the *Sargassum* particles and the PP matrix. This is mainly due to the calcium ions interacting with components of *Sargassum*, mainly alginate, forming interactions that allow *Sargassum* to have an attraction with PP chains [34] and a possible increase in the mobility of polymer chains; there is not a chemical reaction between them. Other reports found that a peak at 1740 cm $^{-1}$ is associated with ester groups of lubricant agents that can react with coupling agents used to improve the interaction between the PP matrix and lignocellulosic materials [35], indicating that these interactions diminish the mechanical behavior of composites.

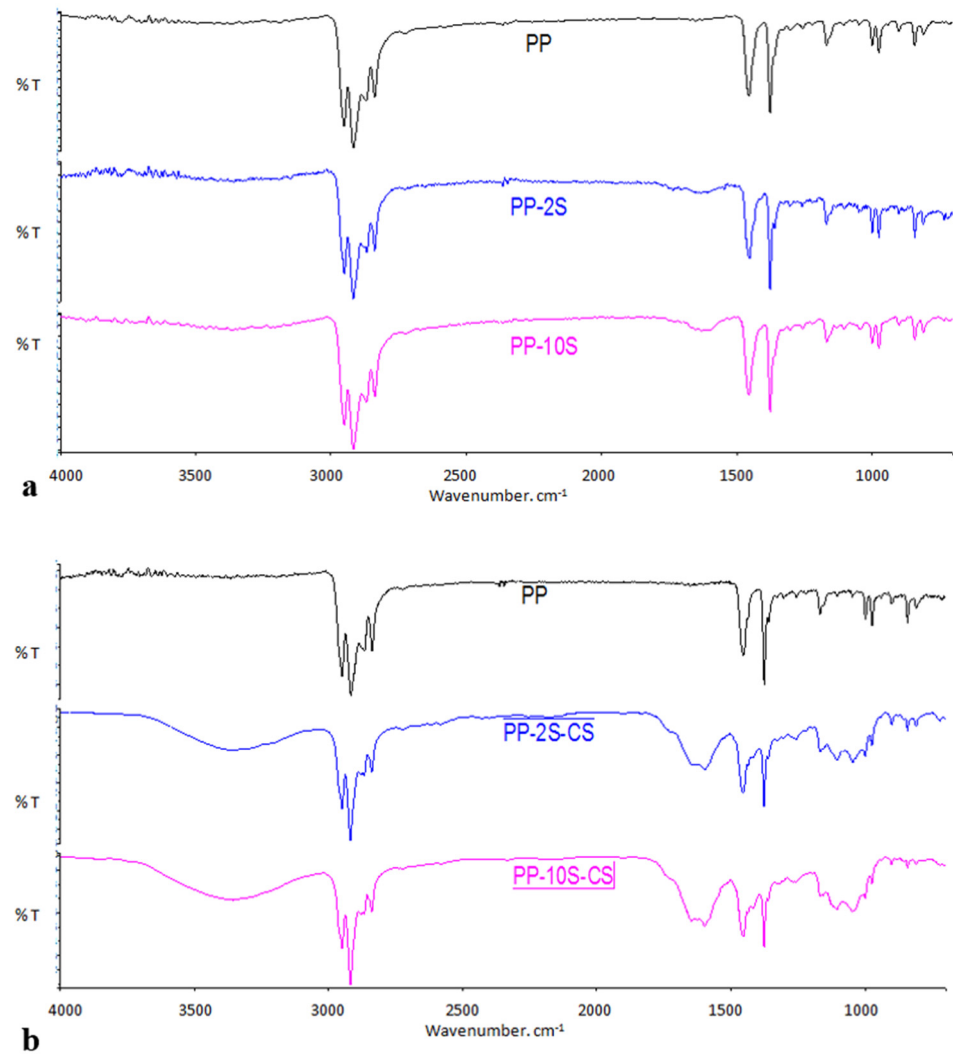


Figure 1. (a) FTIR spectra of PP-S composites. (b) FTIR spectra of PP-S-CS composites.

3.2. Dynamic Mechanical Properties of Composites

Figures 2 and 3 show the DMA thermograms of the storage modulus (E') and $\tan \delta$, respectively, for the neat PP and the PP-S and PP-S-CS composites. Figure 2a shows DMA thermograms of the storage modulus for all PP-S composites without CS. It can be observed that the addition of *Sargassum* particles has a positive effect on the storage modulus because the value of the storage modulus increases, and it reaches its highest value for the composite with a *Sargassum* particle content of 4 phr. Then, the storage modulus decreases as the *Sargassum* content increases. An increase in the value of the storage modulus is associated with good adhesion between *Sargassum* particles and the PP matrix, reflected in the higher stiffness compared to neat PP. This indicates the reinforcing effect of *Sargassum* particles [36–38], which is due to the chain mobility decreasing when *Sargassum* particles are present, as these provide a higher capacity to support stress without deformation [39–41].

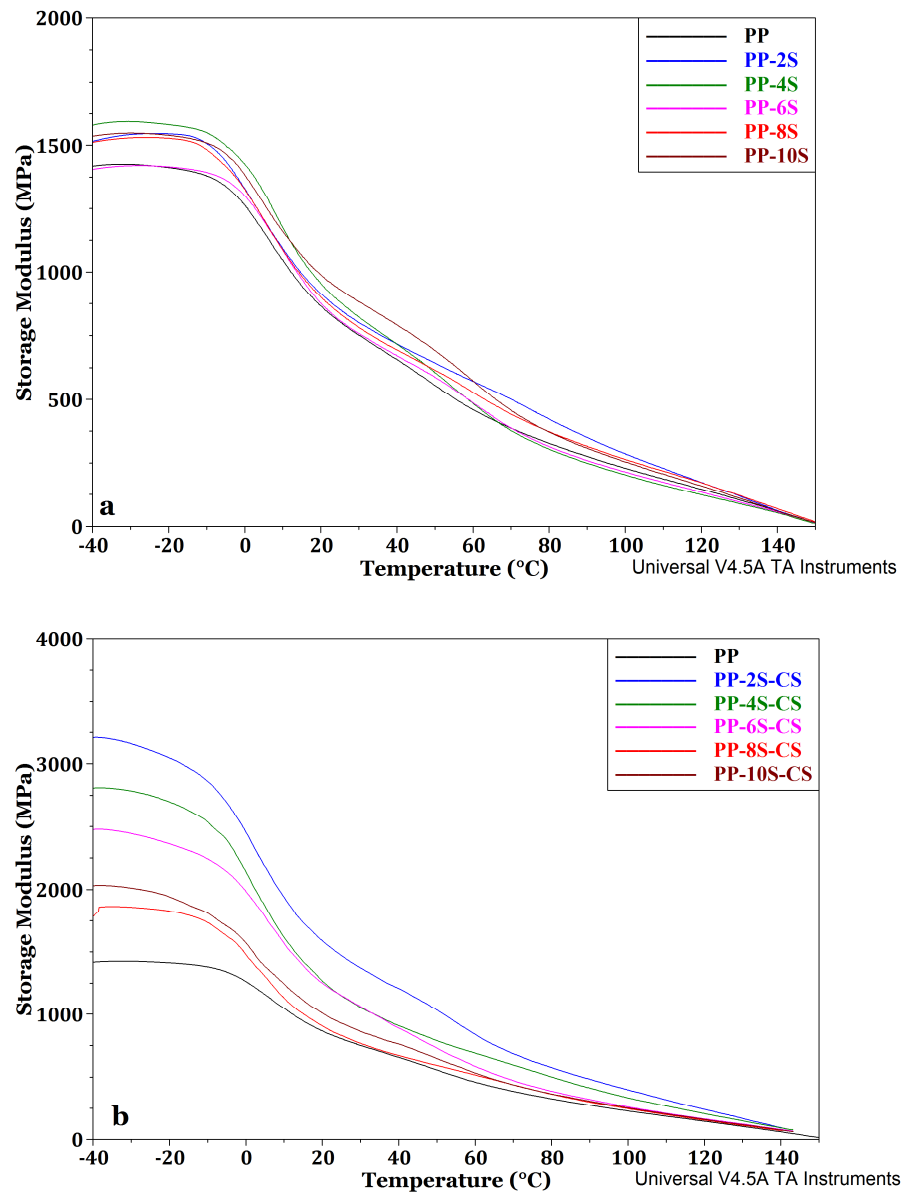


Figure 2. DMA thermograms: (a) storage modulus of PP-S composites; (b) storage modulus of PP-S-CS composites.

On the other hand, Figure 2b not only shows that the storage modulus for PP-S-CS composites increased compared to that for neat PP and PP-S composites without CS but also shows that the storage modulus is much higher compared to that for those composites, reaching a higher storage modulus value for composites with lower *Sargassum* content, and this value decreases when *Sargassum* increases. This increase in storage modulus is indicative of a material that has a better capacity to support stress without deformation. So, as discussed previously, the presence of *Sargassum* particles decreases the polymer chains' mobility. In another way, the increased value of the storage modulus and subsequent decrease thereof are attributed to the fact that there is a saturation of *Sargassum* particles in the PP matrix. This can be discussed and corroborated with a discussion of $\tan \delta$ signal. The significant increase in storage modulus can be due to the CS reducing friction due to its lubricant effect, increasing the reinforcing effect imparted by *Sargassum* particles [18]. So, according to these results, we need to consider that there is a percolation limit to the amount of particles that can be added to obtain a positive reinforcing effect because, with

high *Sargassum* particle content, there is an agglomeration of particles that is identified in the vitreous region, causing the storage modulus and the composite stiffness to decrease.

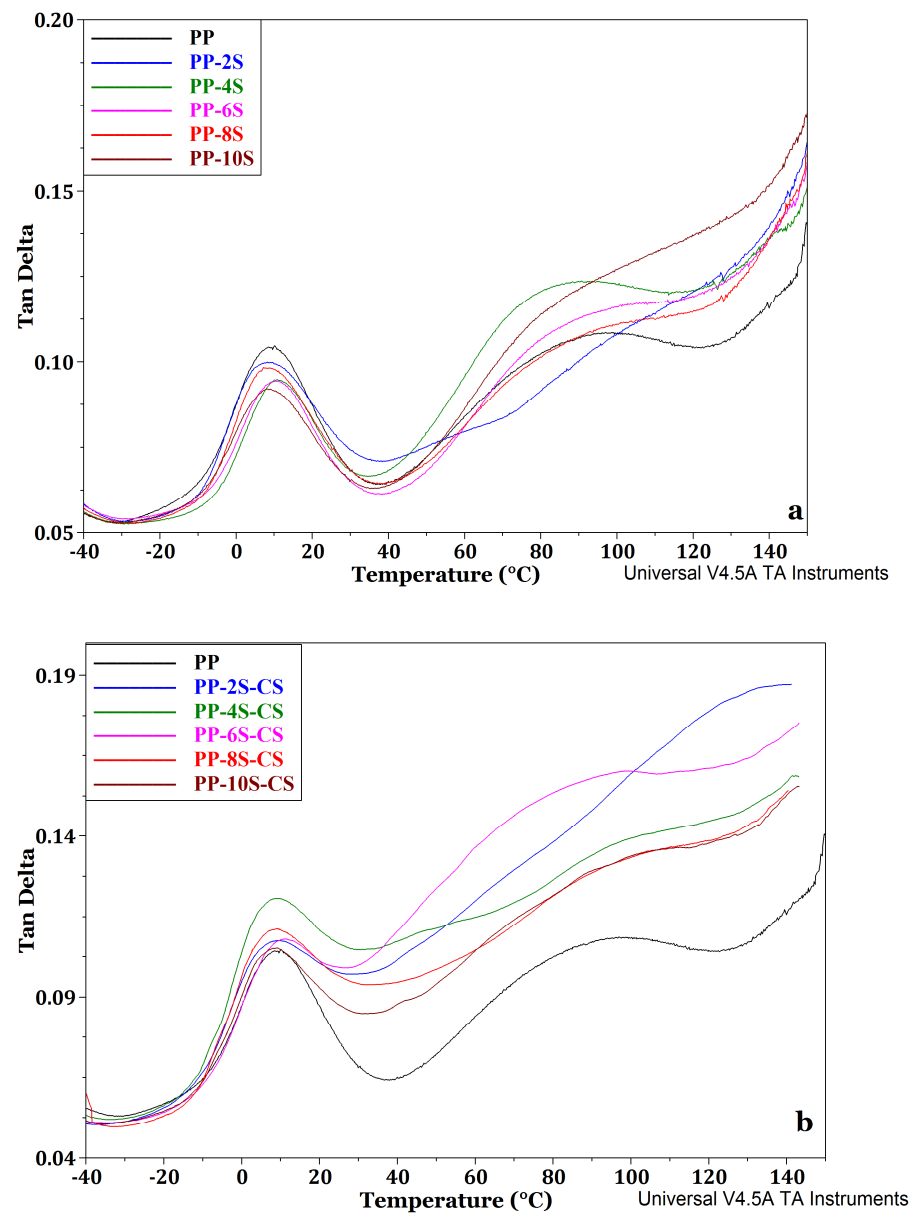


Figure 3. DMA thermograms: (a) $\tan(\delta)$ of PP-S composites; (b) $\tan \delta$ of PP-S-CS composites.

Figure 3a,b show the $\tan \delta$ curves for PP-S and PP-S-CS composites, and two main transitions can be observed. The first transition is around 10 °C at the maximum of the $\tan \delta$ peak, which is associated with glass transition temperature in polymers. It can be observed that the value of the maximum temperature peak does not show significant changes. The T_g values are similar for PP and PP-*Sargassum* composites, so the addition of particles does not have a significant effect on this property. On the other hand, it can be observed that all PP-*Sargassum* composites without CS have a reduction in their $\tan \delta$ peak signal in comparison to the neat PP. This behavior is indicative of the restrained mobility of the polymer chain and indicates that the stiffness of the materials increased. Hence, the interfacial adhesion of the particles to the polymeric matrix was enhanced [20]. The second transition at around 80 °C is associated with the crystalline phase of the polymer. It reflects the laminar and rotational slip mechanism of ordered chains, which in this case decreases the quotient of $\tan \delta$ for PP-*Sargassum* composites, indicating that there is high molecular

disorder compared with neat PP. This is associated with a decrease in crystallinity, which will also be discussed using the DSC and XRD results. Another interesting observation is that the broadness of the $\tan \delta$ peak can be associated with the disparity of the filler. PP–*Sargassum* composites have similar behavior with a broad peak of $\tan \delta$, which can be associated with a non-homogeneous dispersion of the *Sargassum* particles and a possible agglomeration of particles. When CS is added to composites, the first transition peak shows that all the composites have a lower quotient for the $\tan \delta$ peak. As discussed previously, this is indicative of better interfacial adhesion between *Sargassum* particles and the PP matrix. This improvement is due to the presence of CS that reduces the friction, causing a positive reinforcing effect [18].

3.3. Thermal Behavior of Composites (TGA and DSC)

The TGA technique is widely used to evaluate the thermal stability of polymers and composites. Figure 4 shows the TGA thermograms for *Sargassum* particles. It shows that initially, weight loss is associated with moisture loss from the particles between 50 and 150 °C. After that, the DTG curve allows us to observe two main decomposition steps of *Sargassum* particles. The first is at around 260 °C and is attributed to hemicellulose, alginate, lignin, and pectin compounds [36,42]. The second one is at about 320 °C, and it is associated with cellulose decomposition. These results differ slightly from those of a previous work that reported that the thermal decomposition of *Sargassum* starts at a lower temperature. The difference is mainly associated with the kind of *Sargassum*. This previous work reported on the red kind, while our work studied the brown kind. According to Figure 5, the residue is around 30% wt, which is similar to the values reported before [43].

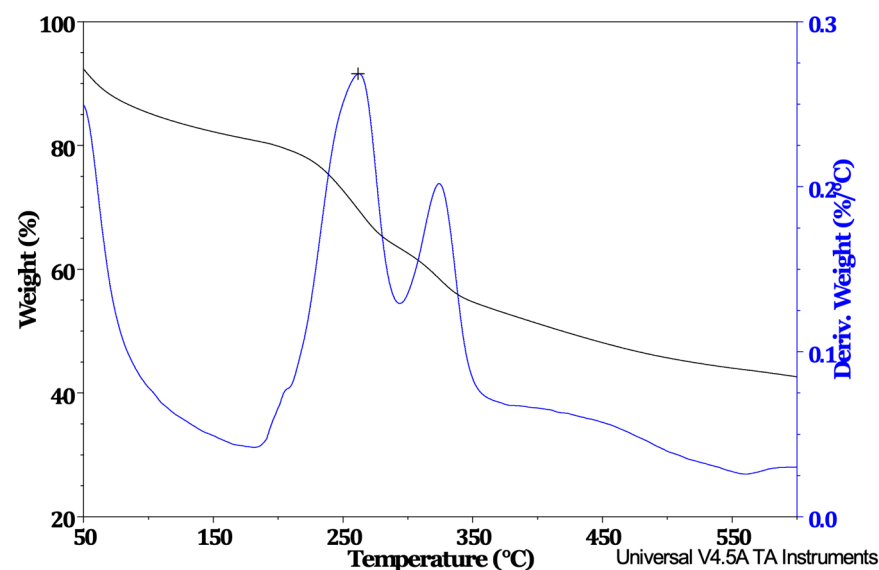


Figure 4. TGA and DTGA thermograms of *Sargassum* particles.

Figure 5 shows the degradation of the composites as a function of the temperature. It is possible to identify that PP–*Sargassum* composites start their decomposition at lower temperatures compared with pristine PP. This behavior is associated with the presence of organic material, as discussed previously. It shows decomposition between 250 and 350 °C. So, the presence of *Sargassum* particles decreased the thermal stability of the composites. This behavior was also noted by Nayak et al. [20] and Wechsler-Pizarro et al. [44] with the addition of lignocellulosic material into PP composites. Additionally, all composites have a wt% residue larger than the neat PP because the interaction between the particles and the matrix has an insulating effect of the residual char that protects the remaining composite from further thermal degradation, as reported previously [18,45]. On the other side, when CS is added to PP–*Sargassum* particle composites, the behavior does not show a significant

change. The onset in TG curves starts at a lower temperature, indicating that the material is losing weight before the neat PP, which is related to the decrease in thermal stability.

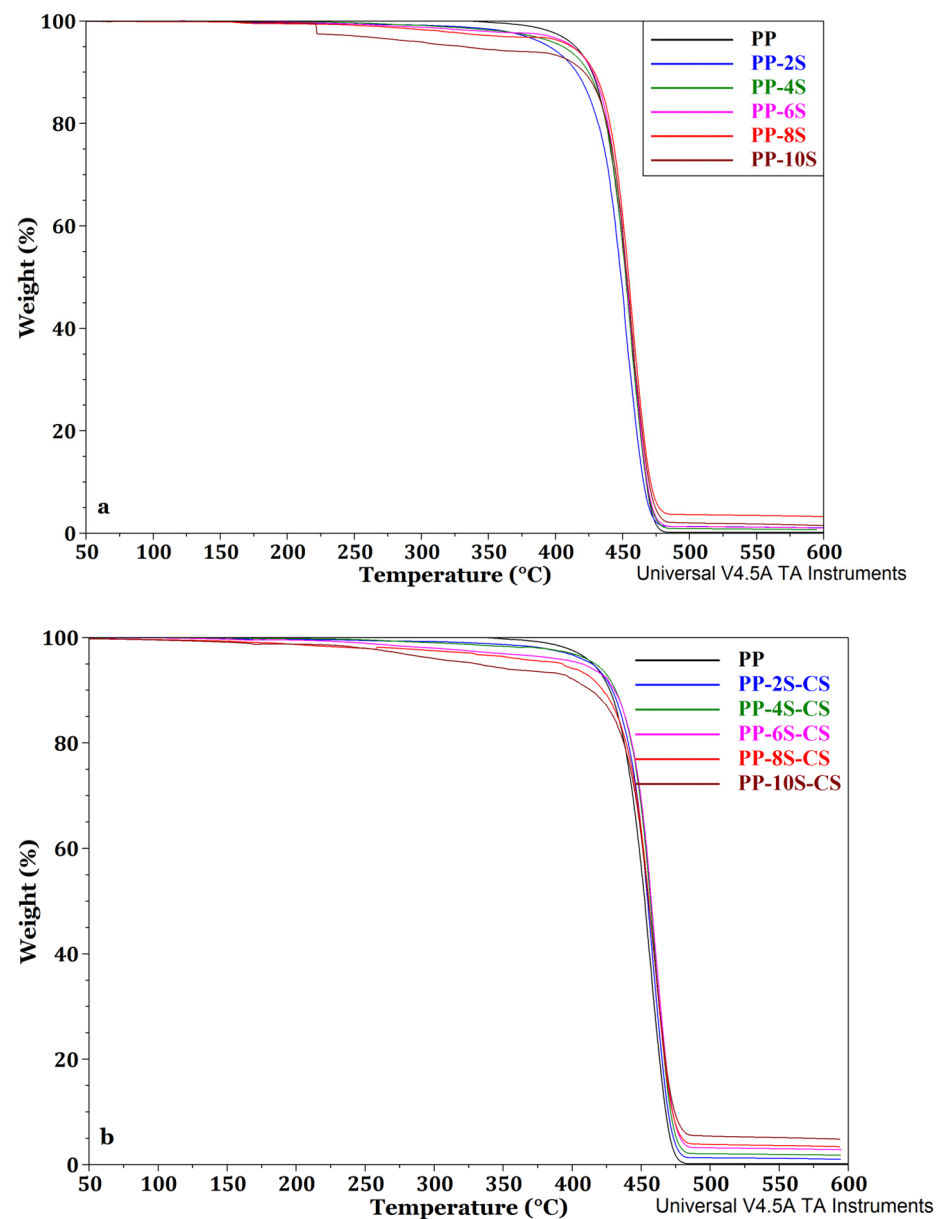


Figure 5. TGA thermograms: (a) weight loss thermogram of PP-S composites; (b) weight loss thermogram of PP-S-CS composites.

Using the derivative curve of TGA, it is possible to identify the main decomposition step at around 450 °C for PP and PP-*Sargassum* particle composites without and with CS. The Supplementary Information includes the DTGA curves for PP-S and PP-S-CS composites. Table 2 reports the values of the average decomposition temperature and decomposition rate ($d(w\%/^{\circ}\text{C})$). It can be seen that the addition of CS caused the average decomposition temperature to increase slightly; the average decomposition temperatures of the composites without CS remain unaffected. In terms of the degradation rate, for composites in which only *Sargassum* particles were added, only PP-2S showed a significant reduction, meaning that the composite lost weight slowly compared with pristine PP, and this also can be associated with the composite reinforcement. For the composites in which CS was added, only those with high CS concentrations (PP-8S-CS and PP-10S-CS) showed a significant reduction in their decomposition rate.

Table 2. Decomposition temperature and derivative value of decomposition for PP-S and PP-S-CS composites.

Composite	T_d ($^{\circ}\text{C}$)	$d(w\%/^{\circ}\text{C})$
PP	456	2.861
PP-2S	452	2.702
PP-4S	456	2.898
PP-6S	454	2.861
PP-8S	457	2.886
PP-10S	455	2.847
PP-2S-CS	456	2.960
PP-4S-CS	459	3.096
PP-6S-CS	459	3.029
PP-8S-CS	459	2.687
PP-10S-CS	460	2.545

Figure 6 shows the typical DSC thermogram for pristine PP where all the thermal transitions can be observed in the first heating cycle; the melting, which was not used to report the ΔH_m ; the quenching cycle; the crystallization, where the ΔH_c was calculated; and the second heating cycle from which the ΔH_m for pristine PP and all PP-S and PP-S-CS composites was taken. The melting temperature (T_m), crystallization temperature (T_c), and crystallinity degree (X_c) of the composites are reported in Table 3. T_m and T_c are considered to be the peaks of the melting and crystallization temperatures, respectively; X_c was calculated using Formula (1).

The values of T_m and T_c for PP are similar to those previously reported in the literature, 165 $^{\circ}\text{C}$ and 112 $^{\circ}\text{C}$, respectively [3]. The T_m value was slightly reduced for PP-S composites with variation around 3–4 $^{\circ}\text{C}$, which can be considered insignificant, while T_c was slightly reduced for PP-S composites. The addition of CS did not have an important effect on T_m and T_c values. In general, it can be observed that the crystallization process is not significantly affected by the presence of *Sargassum* particles. However, the crystallinity degree decreases when *Sargassum* particles are added, and there is no change in this tendency with the addition of CS. In fact, the lowest X_c value was found for the composites with CS added. This behavior can be attributed to the presence of *Sargassum* particles interrupting the order and crystallization of the PP matrix [20]. A different behavior was reported by Rojas-Lema et al. [46]. They found that this was due to the addition of additives such as compatibilizers increasing the interfacial adhesion of lignocellulosic particles and the polymeric matrix increasing the crystallinity.

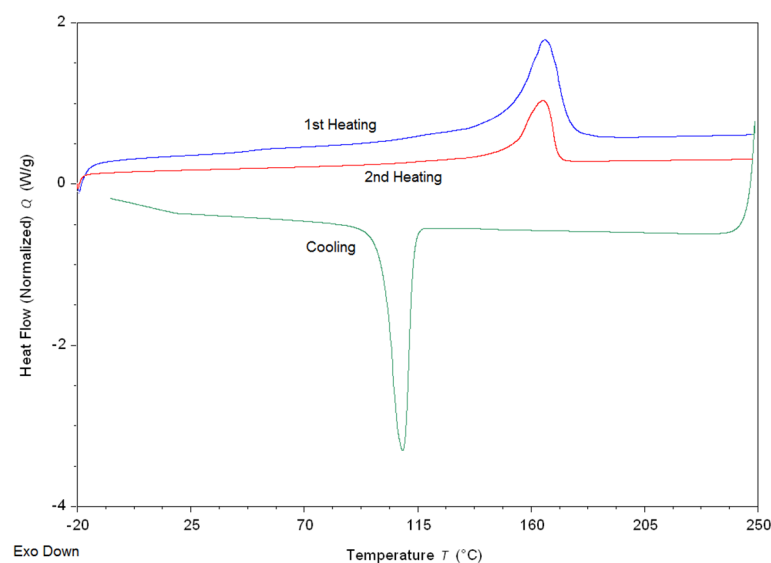
**Figure 6.** Typical DSC thermogram for pristine PP.

Table 3. T_m , T_c , ΔH_m , ΔH_c , and X_c values for PP-S and PP-S-CS composites obtained from DSC.

Composite	T_m (°C)	ΔH_m (J/g)	T_c (°C)	ΔH_c (J/g)	X_c (%)
PP	164	61.101	111	78.24	29.5
PP-2S	161	63.797	113	83.276	30.8
PP-4S	165	59.073	109	76.879	28.5
PP-6S	162	58.371	113	79.961	28.2
PP-8S	163	67.527	112	83.204	32.6
PP-10S	161	56.328	114	74.459	27.2
PP-2S-CS	165	51.310	109	73.749	24.8
PP-4S-CS	165	62.517	109	81.427	30.2
PP-6S-CS	164	58.013	111	74.045	28.0
PP-8S-CS	164	54.190	110	69.247	26.2
PP-10S-CS	164	44.010	110	58.066	21.3

The results show a different behavior from what was previously reported by our research group [37,41]. In those studies, we found T_c values of around 124 °C and T_m values of approximately 174 °C. The main difference concerns the melt flow of the PP matrix. Additionally, the reported X_c value is higher than the values found in those works (by around 40%). This is indicative that the crystallinity and the crystallization process of PP composites depend on the type of lignocellulosic source because the content of cellulose, lignin, and hemicellulose can vary. In the case of *Sargassum*, some other polysaccharides are present in its chemical composition, such as pectin, xylan, xanthan, alginic acids, and chitin [31]. Furthermore, the PP melt flow value also plays an important role in these properties.

3.4. Characterization of Composites by XRD

The X-ray diffraction patterns of the composites are depicted in Figure 7, and the crystallinity degree results are summarized in Table 4. The crystallinity degree was calculated with Formula (2) (Section 2.3).

In Figure 7a, it is possible to identify the characteristic peaks for PP at 2θ 14°, 17°, 18°, and 26°. These are related to the monoclinic structure of the α form of PP with the planes (110), (040), (130), and (060) [47]. Additionally, peaks at 21.5° and 22.5°, due to the planes α (111) + β (311) and α (311) + β (041), are also characteristic of PP [48]. For the PP-S composite, it is possible to identify a displacement to lower angles. This indicates that *Sargassum* particles penetrate the PP structure and increase the basal space in the polymer chains. The addition of CS (Figure 7b) does not have a considerable effect on the characteristic peaks observed for PP-*Sargassum* composites.

Table 4 shows that only low-concentration composites have a higher crystallinity than neat PP. The same can be observed for composites with CS. The peaks of the composites are located at the same angles as the peaks of PP (14°, 17°, 18.5°, 21°, and 22°). As in the DSC tests, increasing the *Sargassum* particle concentration caused the composites to have lower crystallinity values. According to the results, only lower *Sargassum* particle contents cause the crystallinity to increase, and higher contents, up to 4 phr, have a negative effect on the crystallinity percentage. There are reports that the addition of CS generates vitreous agglomerates with a lamella-ordered structure, which means that the crystallinity process is affected by the presence of a CS-generated β -phase, which is not the case in our work [22].

The observed crystallinity content of PP is lower than that in other reports [49]. The main difference is in the lower melt flow index value for the PP used. The lower value of this property is associated with higher molecular weight and poor mobility of polymer chains. In contrast, when the melt flow value is higher, the PP matrix has better molecular mobility, reflecting a decrease in crystallinity.

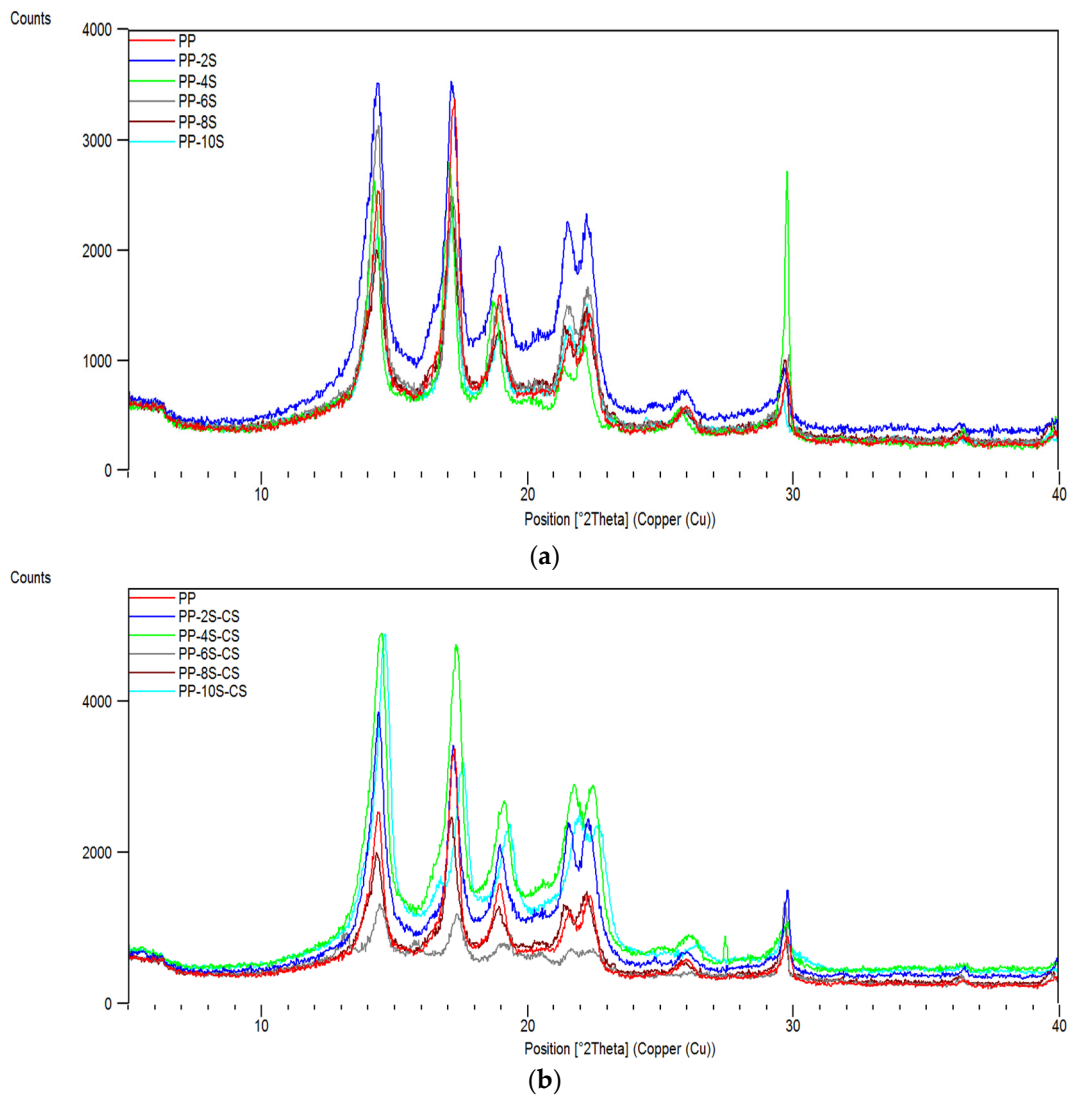


Figure 7. (a) X-ray patterns for PP and PP-S composites. (b) X-ray patterns for PP-S-CS composites.

Table 4. Calculation of crystallinity grade for PP-S and PP-S-CS composites.

Composite	Ac	Ac + Aa	Xc, %
PP	5015.65	19,198.02	26.13
PP-2S	8087.94	27,034.82	29.92
PP-4S	5215.40	18,659.35	27.95
PP-6S	4743.28	20,630.02	22.99
PP-8S	4778.30	19,920.89	23.99
PP-10S	3863.36	18,647.51	20.72
PP-2S-CS	7443.70	26,201.84	28.41
PP-4S-CS	11,462.16	36,177.35	31.68
PP-6S-CS	2597.79	17,093.53	15.20
PP-8S-CS	4778.30	19,920.89	23.99
PP-10S-CS	8520.59	34,214.37	24.90

4. Conclusions

The present work opens a new possibility for using *Sargassum* particles as a natural additive in a polymer matrix. It is an interesting and economically and environmentally attractive option because these particles in low content can enhance the properties of the polymer matrix and reduce the production cost of adding commercial fillers. Furthermore,

this method can help solve a significant problem on the Caribbean coast caused by *Sargassum*. The results clearly show that using CS as an additive enhanced the adhesion of the *Sargassum* particles to the PP matrix, as shown by the FTIR results. The DMA results show that the addition of *Sargassum* particles at low content has a positive effect on storage modulus, improving rigidity. Still, when CS is added, there is a significant increase, more than twice compared with that of PP–*Sargassum* composites without CS. This is attributed to the mobility of the polymer chains that decreases when *Sargassum* particles are added. The PP–*Sargassum* composites without and with CS show lower thermal stability, beginning their decomposition at around 250 °C, which is lower than pristine PP. The DSC and XRD results agree and show that, for lower concentrations, a higher crystallinity than that of neat PP can be achieved. *Sargassum*-reinforced composites are recommended for industrial applications as long as the concentrations of *Sargassum* particles are kept low, i.e., 2 phr. To achieve even better properties, the addition of CS is recommended. In this case, the best formulation found in this study was at 4 phr with 1%wt of CS.

Other studies revealed that the mechanical properties depend on the filler/matrix interface. For this reason, further studies on the chemical treatment of the surface of the *Sargassum* particles may show a way to improve the interaction between the polymer matrix and particles.

Supplementary Materials: The following supporting information can be downloaded at: <https://www.mdpi.com/article/10.3390/jcs7110455/s1>, Figure S1. DTGA thermograms for PP-S composites; Figure S2. DTGA thermograms for PP-S-CS composites; Figure S3. IR spectra for PP, and PP-S composites; Figure S4. IR spectra for PP, and PP-S-CS composites; Table S1. Density of PP-S composites and PP-S-CS composites. Reference [50] is cited in the supplementary materials.

Author Contributions: Conceptualization, J.D.A.-V., B.A.S.-C., M.Y.C.-C. and J.L.R.-A.; methodology, J.D.A.-V., B.A.S.-C. and A.C.E.-F.; software, M.Y.C.-C., B.A.S.-C. and J.L.R.-A.; validation, M.Y.C.-C., J.L.R.-A. and B.A.S.-C.; formal analysis, A.C.E.-F., J.L.R.-A. and B.A.S.-C.; investigation, J.D.A.-V., J.L.R.-A. and B.A.S.-C.; resources, J.L.R.-A. and B.A.S.-C.; data curation, M.Y.C.-C. and J.D.A.-V.; writing—original draft preparation, J.D.A.-V., J.L.R.-A. and B.A.S.-C.; writing—review and editing, J.L.R.-A. and B.A.S.-C.; visualization, M.Y.C.-C.; supervision, J.L.R.-A.; project administration, M.Y.C.-C.; funding acquisition, J.L.R.-A. and B.A.S.-C. All authors have read and agreed to the published version of the manuscript.

Funding: This research was funded by Tecnológico Nacional de México, grant number 10164.21-P.

Data Availability Statement: Publicly available datasets were analyzed in this study. This data can be found here: <https://rinacional.tecnm.mx/handle/TecNM/832> (accessed on 1 September 2023).

Acknowledgments: One of authors (J.D.A.-V.) wish to thanks to CONACYT for grant number 786568, authors would like to thank; Indelpro S.A. de C.V., Altamira, Tamps. for their kind donation of the polymer resins and their assistance with the DSC analyses, and Katherine Monserrath Maya-Ruiz for her contribution to the preparation of the CS composite materials and their testing, and the APC was funded by the authors. This research was carried out in the postgraduate in Master Science in Chemical Engineering (MCIQ).

Conflicts of Interest: The authors declare no conflict of interest.

References

1. Alsaadi, M.; Erklig, A.; Albu-khaleefah, K. Effect of pistachio shell particle content on the mechanical properties of polymer composite. *Arab. J. Sci. Eng.* **2018**, *43*, 4689–4696. [[CrossRef](#)]
2. Valvez, S.; Maceiras, A.; Santos, P.; Reis, P.N.B. Olive Stones as filler for polymer-based composites: A review. *Materials* **2021**, *14*, 845. [[CrossRef](#)]
3. Bazan, P.; Salasinska, K.; Kuciel, S. Flame retardant polypropylene reinforced with natural additives. *Ind. Crops Prod.* **2021**, *164*, 113356. [[CrossRef](#)]
4. Barczewski, M.; Mysiukiewicz, O.; Kloziński, A. Complex modification effect of linseed cake as an agricultural waste filler used in high density polyethylene composites. *Iran. Polym. J.* **2018**, *27*, 677–688. [[CrossRef](#)]
5. Chun, K.S.; Maimunah, T.; Yeng, C.M.; Yeow, T.K.; Kiat, O.T. Properties of Corn Husk Fibre Reinforced Epoxy Composites Fabricated Using Vacuum-assisted Resin Infusion. *J. Phys. Sci.* **2020**, *31*, 17–31. [[CrossRef](#)]

6. Hristov, V.N.; Krumova, M.; Vasileva, S.T.; Michler, G.H. Modified polypropylene wood flour composites. II. Fracture, deformation, and mechanical properties. *J. Appl. Polym. Sci.* **2004**, *92*, 1286–1292. [[CrossRef](#)]
7. Cuéllar, A.; Muñoz, I. Fibra de Guadua como refuerzo de matrices poliméricas. *Dyna* **2010**, *77*, 137–142.
8. Kuciel, S.; Bazan, P.; Nosal, P.; Wierzbicka-Miernik, A. A novel hybrid composites based on biopolyamide 10.10 with basalt/aramid fibers: Mechanical and thermal investigation. *Compos. Part B Eng.* **2021**, *223*, 109125.
9. Godínez-Ortega, J.L.; Cuatlán-Cortés, J.V.; López-Bautista, J.M.; van Tussenbroek, B.I. A Natural History of Floating *Sargassum* species (Sargasso) from Mexico. In *Natural History and Ecology of Mexico and Central America*; Hufnagel, L., Ed.; IntechOpen: London, UK, 2021.
10. Rossignolo, J.A.; Duran, A.J.F.P.; Bueno, C.; Martinelli Filho, J.E.; Junior, H.S.; Tonin, F.G. Algae application in civil construction: A review with focus on the potential uses of the pelagic *Sargassum* spp. biomass. *J. Environ. Manag.* **2022**, *303*, 114258. [[CrossRef](#)]
11. Rabemanolontsoa, H.; Saka, S. Comparative study on chemical composition of various biomass species. *RSC Adv.* **2013**, *3*, 3946–3956. [[CrossRef](#)]
12. Salazar-Cruz, B.A.; Zapien-Castillo, S.; Hernández-Zamora, G.; Rivera-Armenta, J.L. Investigation of the performance of asphalt binder modified by *Sargassum*. *Constr. Build. Mater.* **2021**, *271*, 121876. [[CrossRef](#)]
13. García-Castañeda, J.L.; Salazar-Cruz, B.A.; Hernández-Zamora, G.; Rivera-Armenta, J.L.; Flores-Hernández, C.G.; Espindola-Flores, A.C. Obtaining and characterization of a composite material with SBS and *Sargassum* particles. *MRS Adv.* **2022**, *7*, 987–990. [[CrossRef](#)]
14. Sorieul, M.; Thumm, A.; Risani, R.; Dickson, A. Ligno-cellulosic fibre sized with nucleating agents promoting transcrystallinity in isotactic polypropylene composites. *Materials* **2020**, *13*, 1259.
15. Venkatachalam, C.D.; Anbupalani, M.S.; Rathanasamy, R. Influence of coupling agent on altering the reinforcing efficiency of natural fibre-incorporated polymers—A review. *J. Reinf. Plast. Compos.* **2020**, *39*, 520–544.
16. Vinod Kumar, T.; Chandraskaran, M.; Santhanam, V.; Sudharsan, V.D. Effect of coupling agent on mechanical properties of palm petiole nanofiber reinforced composite. *IOP Conf. Ser. Mater. Sci. Eng.* **2017**, *183*, 012006. [[CrossRef](#)]
17. Hussain, M.; Nakahira, A.; Nishijima, S.; Niihara, K. Effects of coupling agents on the mechanical properties improvement of the TiO₂ reinforced epoxy system. *Mater. Lett.* **1996**, *26*, 299–303. [[CrossRef](#)]
18. Panin, C.V.; Kornienko, L.A.; Suan, T.N.; Ivanova, L.R.; Poltaranin, M.A. The effect of adding calcium stearate on wear-resistance of ultra-high molecular weight polyethylene. *Procedia Eng.* **2015**, *113*, 490–498. [[CrossRef](#)]
19. Suter, U.W.; Osman, M.A.; Atallah, A. Influence of excessive filler coating on the tensile properties of LDPE-calcium carbonate composites. *Polymer* **2004**, *45*, 1177–1183.
20. Nayak, S.; Mohanty, S.; Samal, S.K. Influence of short bamboo/glass fiber on the thermal, dynamic mechanical and rheological properties of polypropylene hybrid composites. *Mater. Sci. Eng. A* **2009**, *523*, 32–38. [[CrossRef](#)]
21. Bensaad, F.; Belhaneche-Bensemra, N. Effects of calcium stearate as pro-oxidant agent on the natural aging of polypropylene. *J. Polym. Eng.* **2018**, *38*, 715–721. [[CrossRef](#)]
22. Zhang, X.; Wei, F.; Wang, Z.; Li, G.; Yang, S.; Feng, J. Comparative investigation of the structural evolution of zinc stearate and calcium stearate in a polypropylene random copolymer upon heating and cooling. *Polymer* **2023**, *267*, 125646. [[CrossRef](#)]
23. Bhowmick, M.; Mukhopadhyay, S.; Alagirusamy, R. Mechanical properties of natural fibre-reinforced composites. *Text. Prog.* **2012**, *44*, 85–140. [[CrossRef](#)]
24. Ramazani, S.A.; Rahimi, A.; Frounchi, M.; Radman, S. Investigation of flame retardancy and physical–mechanical properties of zinc borate and aluminum hydroxide propylene composites. *Mater. Des.* **2008**, *29*, 1051–1056. [[CrossRef](#)]
25. Lin, Y.; Chen, H.; Chan, C.M.; Wu, J. Nucleating effect of calcium stearate coated CaCO₃ nanoparticles on polypropylene. *J. Colloid Interface Sci.* **2011**, *354*, 570–576. [[CrossRef](#)] [[PubMed](#)]
26. Feng, J.; Chen, M.; Huang, Z.; Guo, Y.; Hu, H. Effects of Mineral Additives on the α -Crystalline Form of Isotactic Polypropylene. *J. Appl. Polym. Sci.* **2002**, *85*, 1742–1748. [[CrossRef](#)]
27. Qiu, W.; Mai, K.; Zeng, H. Effect of macromolecular coupling agent on the property of PP/GF composites. *J. Appl. Polym. Sci.* **1999**, *71*, 1537–1542. [[CrossRef](#)]
28. Chun, K.S.; Husseinsyah, S.; Yeng, C.M. Green composites from kapok husk and recycled polypropylene: Processing torque, tensile, thermal, and morphological properties. *J. Thermoplast. Compos. Mater.* **2016**, *29*, 1517–1535. [[CrossRef](#)]
29. Doh, H.; Dunno, K.D.; Whiteside, W.S. Preparation of novel seaweed nanocomposite film from brown seaweeds *Laminaria japonica* and *Sargassum natans*. *Food Hydrocoll.* **2020**, *105*, 105744. [[CrossRef](#)]
30. Chun, K.S.; Husseinsyah, S.; Osman, H. Modified Cocoa Pod Husk-Filled Polypropylene Composites by Using Methacrylic Acid. *BioResources* **2013**, *8*, 3260–3275.
31. Apaydin, G.; Aylikci, V.; Cengiz, E.R.H.A.N.; Saydam, M.; K p, N.; Tiraşođlu, E. Analysis of metal contents of seaweed (*Ulvalactuca*) from Istanbul, Turkey by EDXRF. *Turk. J. Fish. Aquat. Sci.* **2010**, *10*, 215–220. [[CrossRef](#)]
32. Escobar-Medina, F.J.; Rivera-Armenta, J.L.; Hernández-Zamora, G.; Salazar-Cruz, B.A.; Zapien-Castillo, S.; Flores-Hernández, C.G. *Sargassum*-Modified Asphalt: Effect of Particle Size on Its Physicochemical, Rheological, and Morphological Properties. *Sustainability* **2021**, *13*, 11734. [[CrossRef](#)]
33. Lamont, K.; Pensini, E.; Marangoni, A.G. Gelation on demand using switchable double emulsions: A potential strategy for the in situ immobilization of organic contaminants. *J. Colloid Interface Sci.* **2020**, *562*, 470–482. [[CrossRef](#)] [[PubMed](#)]

34. Quan, W.; Li, P.; Wei, J.; Jiang, Y.; Liang, Y.; Zhang, W.; Ouyang, Q. Bio-Multifunctional Sponges Containing Alginate/Chitosan/*Sargassum* Polysaccharides Promote the Healing of Full-Thickness Wounds. *Biomolecules* **2022**, *12*, 1601. [[CrossRef](#)] [[PubMed](#)]
35. Bettini, S.H.P.; de Miranda Josefovich, M.P.P.; Muñoz, P.A.R.; Lotti, C.; Mattoso, L.H.C. Effect of lubricant on mechanical and rheological properties of compatibilized PP/sawdust composites. *Carbohydr. Polym.* **2013**, *94*, 800–806. [[CrossRef](#)]
36. Salasinska, K.; Ryszkowska, J. The effect of filler chemical constitution and morphological properties on the mechanical properties of natural fiber composites. *Compos. Interfaces* **2015**, *22*, 39–50. [[CrossRef](#)]
37. Rivera-Armenta, J.L.; Salazar-Cruz, B.A.; Espindola-Flores, A.C.; Villarreal-Lucio, D.S.; De León-Almazán, C.M.; Estrada-Martinez, J. Thermal and thermomechanical characterization of Polypropylene-seed shell particles composites. *Appl. Sci.* **2022**, *12*, 8336. [[CrossRef](#)]
38. Rajan, R.; Rainosal, E.; Ramamoorthy, S.M.; Thomas, S.P.; Zavasnik, J.; Vuorinen, J.; Skrifvars, M. Mechanical, Thermal and Burning properties of viscose fabric composites—Influence of epoxy resin modification. *J. Appl. Polym. Sci.* **2018**, *135*, 46673. [[CrossRef](#)]
39. Ornaghi, H.L., Jr.; Bolner, A.S.; Fiorio, R.; Zattera, A.J.; Amico, S.C. Mechanical and dynamic mechanical analysis of hybrid composites molded by resin transfer molding. *J. Appl. Polym. Sci.* **2010**, *118*, 887–896. [[CrossRef](#)]
40. Rosa, S.M.; Nachtigall, S.M.; Ferreira, C.A. Thermal and dynamic-mechanical characterization of rice-husk filled polypropylene composites. *Macromol. Res.* **2009**, *17*, 8–13. [[CrossRef](#)]
41. Salazar-Cruz, B.A.; Chávez-Cinco, M.Y.; Morales-Cepeda, A.B.; Ramos-Galván, C.E.; Rivera-Armenta, J.L. Evaluation of thermal properties of composites prepared from pistachio shell particles treated chemically and polypropylene. *Molecules* **2022**, *27*, 426. [[CrossRef](#)]
42. Kulig, D.; Zimoch-Korzycka, A.; Jarmoluk, A.; Marycz, K. Study on alginate–chitosan complex formed with different polymers ratio. *Polymers* **2016**, *8*, 167. [[CrossRef](#)] [[PubMed](#)]
43. Ali, I.; Bahadar, A. Red Sea seaweed (*Sargassum* spp.) pyrolysis and its devolatilization kinetics. *Algal Res.* **2017**, *21*, 89–97. [[CrossRef](#)]
44. Wechsler-Pizarro, A.; Nuñez-Decap, M.; Vidal-Vega, M. Mechanical, physical, thermal and morphological properties of polypropylene composite materials developed with particles of peach and cherry stones. *Sustain. Mater. Technol.* **2021**, *29*, e00300.
45. Marcovich, N.E.; Nuñez, A.J.; Kenny, J.M.; Reboredo, M.M.; Aranguren, M.I. Thermal and Dynamic Mechanical characterization of Polypropylene-Woodflour Composites. *Polym. Eng. Sci.* **2002**, *42*, 733–742.
46. Rojas-Lema, S.; Arevalo, J.; Gomez-Caturla, J.; Garcia-Garcia, D.; Torres-Giner, S. Peroxide-Induced Synthesis of Maleic Anhydride-Grafted Poly(butylene succinate) and Its Compatibilizing Effect on Poly(butylene succinate)/Pistachio Shell Flour Composites. *Molecules* **2021**, *26*, 5927. [[CrossRef](#)]
47. Wang, S.; Aji, A.; Guo, S.; Xiong, C. Preparation of microporous polypropylene/titanium dioxide composite membranes with enhanced electrolyte uptake capability via melt extruding and stretching. *Polymers* **2017**, *9*, 110. [[CrossRef](#)]
48. Somani, R.H.; Hsiao, B.S.; Nogales, A.; Fruitwala, H.; Srinivas, A.; Tsou, A.H. Structure development during shear flow induced crystallization of i-PP: In situ Wide-Angle X-ray diffraction study. *Macromolecules* **2001**, *34*, 5902–5909. [[CrossRef](#)]
49. Borysiak, S.; Klapiszewski, Ł.; Bula, K.; Jesionowski, T. Nucleation ability of advanced functional silica/lignin hybrid fillers in polypropylene composites. *J. Therm. Anal. Calorim.* **2016**, *126*, 251–262. [[CrossRef](#)]
50. Amieva, E.J.C.; Velasco-Santos, C.; Martínez-Hernández, A.L.; Rivera-Armenta, J.L.; Mendoza-Martínez, A.M.; Castaño, V.M. Composites from chicken feathers quill and recycled polypropylene. *J. Compos. Mater.* **2015**, *49*, 275–283. [[CrossRef](#)]

Disclaimer/Publisher’s Note: The statements, opinions and data contained in all publications are solely those of the individual author(s) and contributor(s) and not of MDPI and/or the editor(s). MDPI and/or the editor(s) disclaim responsibility for any injury to people or property resulting from any ideas, methods, instructions or products referred to in the content.